Arno Project: Evolution of Data Processing Techniques in Dual Polarization radar

ARNO PROJECT: EVOLUTION OF DATA PROCESSING TECHNIQUES IN DUAL POLARIZATION RADAR

D.Giuli, L. Baldini, L. Facheris, and M. Gherardelli
Department of Electronic Engineering - University of Florence - Italy

1. INTRODUCTION

Weather radars can play the major role in an integrated real-time monitoring system aiming at flash-flood forecasting in short time response basins as the Arno basin (Becchi and Giuli, 1987). Since quality of radar data is degraded by several sources of error, many researches have been developed to devise proper data processing techniques to enhance radar based precipitation estimates and thus improving the effectiveness of a radar based monitoring system. However, results obtained by means of different techniques are difficult to compare since experimental results are always only partially available or obtained in particular or non controllable conditions. In this paper we present an integrated and flexible tool for simulation and analysis of C-band dual polarization radar (Seliga an Bringi, 1976) data, developed to study and optimize proper data processing techniques meeting those hydrological applications requirements, which is one of the major goals of Arno Project. Fig. 1 illustrates the modular development of the simulation and data processing scheme. A storm generation model, whose parameters are set according to a statistical analysis of the long-term records of raingages present in the Arno river basin, is used to generate the input to a radar measurement simulation model which provides dual polarization radar "measured" reflectivity fields. This approach gives the opportunity to compare two space-time precipitation fields: the "ideal" field, generated by the storm generation model, and the corresponding radar measured field, eventually obtained after proper processing. In Section 2 the basic steps of the simulation procedure and its numerical implementation are described. Finally, Section 3 presents some simulation results concerning the test of some data processing techniques.

2. THE SIMULATION PROCEDURE

2.1 The rainfall model

The simulation procedure starts from the "true" ground rainfall field. Such field is generated through a stochastic space-time model developed by Rodriguez-Iturbe and Eagleson (1987), slightly modified for our applications. It characterizes the rainfall event as built up by a random number of rain cells, moving with a common velocity, whose centers are spatially distributed according to a two-dimensional Poisson process defined by five parameters.

2.2 The generation of "ground" reflectivity fields

The generation of "true" reflectivity data has been developed in two steps, first defining a scheme allowing to derive two-dimensional Z_H and Z_{DR} reflectivity fields consistent with the true rainfall fields at ground ("reflectivity fields at ground"). The first problem has been solved by using the exponential DSD model:

$$N(D_{eq}) = N_0 \exp(-\Lambda D_{eq}) \qquad (1)$$

where $\Lambda = 4.1 / R^{0.21}$ and D_{eq}(mm) is the equivolume spherical diameter of a raindrop, as in Marshall and Palmer (1948), but with N_0 given by:

$$N_0 = \frac{88.419\ \Lambda^4\ R}{[9.65 - 10.3/(1 + 0.6/\Lambda)^4]}\ . \qquad (2)$$

Such value can easily be obtained by resorting to the analytical definition of R, using (1) and the expression proposed by Atlas et al. (1973) for the terminal velocity of drops

$$v_t(D_{eq}) = 9.65 - 10.3 \exp(-0.6\ D_{eq}) \quad (m s^{-1}). \qquad (3)$$

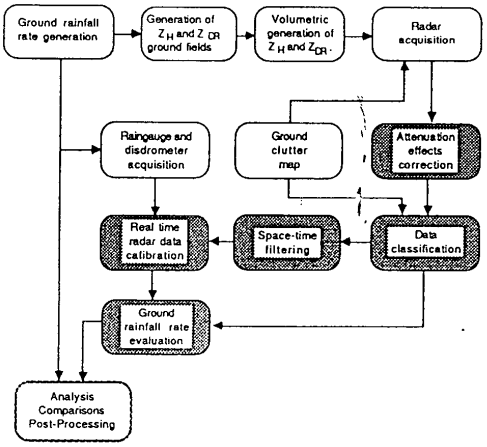

Fig. 1 Scheme of the simulation and processing (shadowed) steps.

Once the DSD parameters are known, it is possible to associate univocally a given R at a location at ground with the absolute and the differential reflectivity expressed in dBZ and dB as $Z_H(dBZ) = 10 \log Z_H\,(mm^6 m^{-3})$ and $Z_{DR}(dB) = 10 \log (Z_H/Z_V)$, respectively. This implies that the resulting relationship between Z_H and Z_{DR} is deterministic, but decidedly contrasts with both experimental measurements and simulations, which clearly indicate that Z_H and Z_{DR} in rain are random variables with a very high degree of correlation (Sachidananda and Zrnić, 1987). Thus, a procedure has to be devised to impose a given spatial correlation between the Z_H and Z_{DR} field at ground. The advantage of the approach we are going to describe here is that no basic hypotheses about the rainfall model are needed, in order to allow a modular development of the simulation procedure. A noise field is added to the Z_{DR} field by adding independent, exponentially distributed quantities, all characterized by the same distribution parameter λ_d to the previously calculated Z_{DR} values. The resulting field, though being characterized by a plausible statistical fluctuation, would present inadequate values of the spatial correlation coefficient, in particular, for spatial lags close to zero. The required spatial correlation pattern is imposed by resorting to a non-recursive spatial filtering made with a 5x5 moving window and applied to the reflectivity samples associated with the radar resolution cells which uses a Gaussian weighting function, whose weights are given by :

$$w(k,l) = \exp(-(k^2 + l^2)/2\sigma^2), \quad k, = -2, \ldots, 2 \qquad (4)$$

with $\sigma = \sqrt{5}$. The reduction of the point standard deviation of the Z_{DR} field, σ_F, can be imposed by setting a proper value of σ_d. Simulation by Sachidananda and Zrnić (1987) showed that the spread of Z_{DR} is practically independent of Z_H. Assuming this

the Z_{DR} field is uniformly distributed with a maximum scatter of Z_{DR} about 1 dB, we suppose $\sigma_F = 1/\sqrt{12}$ dB. The corresponding value of λ_d is thus evaluated by:

$$\lambda_d = \frac{1}{\sigma_n} \simeq \frac{0.366}{\sigma_F} \simeq 1.27 \ \text{dB}^{-1}, \qquad (5)$$

σ_n being $\sigma$the sample standard deviation of the added "noise" field. Since filtering alters the original bond among reflectivity fields and rainfall field, it is necessary to recompute a Z_H field physically consistent with Z_{DR} and R. Given R and Z_{DR}, Z_H has been obtained by applying the relationship experimentally derived by Seliga et al. (1986):

$$R = 1.51 \cdot 10^{-3} \, Z_H \, Z_{DR}^{-1.55} \quad (\text{mm h}^{-1}) \qquad (6)$$

where Z_H is in mm^6m^{-3} and Z_{DR} in dB. As can be easily verified, this has no effect on the scatter of Z_{DR} about Z_H.

2.3 Generation of volumetric Z_{DR} and Z_H fields

The two-dimensional reflectivity fields at ground, are developed along a vertical coordinate axis in order to generate a couple of volumetric field. These can be thought as made up by cubic cells (called here "spatial resolution cells") supposed to present uniform reflectivities. Volume resolution of such cells has been fixed as $10^{-3}\,\text{Km}^3$, sufficient to account for the small scale variations of reflectivity. Various models of vertical profiles could be adopted, but since critical events on the Arno basin are more likely to be of the stratiform type than of the convective one, the vertical profiles that have been simulated fit in a basic pattern ("medium profile") evidencing the presence of a melting layer at an altitude varying from one medium profile to another. The height of the melting layer, in fact, varies spatially also in the same event, depending on the rainfall intensity at ground and not only from storm to storm. Since detailed vertical profile measurements are not currently available for the Arno basin, Z_{DR} and Z_H vertical profiles are chosen according to the results presented by Hall et al. (1984) with the height of Z_H peak at 1.3 Km. Slight variations in the shape of the profiles are introduced by adding a certain degree of randomness in the amplitude of the Z_H peak and fluctuations about the medium profiles.

2.5 Simulation of the radar acquisition process

In order to realistically simulate the acquisition of Z_H and Z_{DR} radar measurement data, the volume integration process involved in radar measurements has now to be modeled. This requires that the spatial resolution cell is identified within each radar sample volume. Reflectivities fluctuations in each resolution cell are simulated according to an exponential distribution and assuming that the Z_H and Z_V values in each cell are the mean values of the distribution (Doviak and Zrnić, 1984). Beam smoothing effect is then taken into account. The integration of N_i pulses within the beamwidth for each polarization channel is then simulated by considering the square law and the logarithmic receivers. The parameters needed for the proposed radar acquisition model are the radar site height h_s, the beam elevation ϵ, the azimuth beam-width Φ_l, the elevation beam-width Φ_r, and the range resolution Δr. The effects of propagation attenuation at C-band have also been simulated. For this purpose, the specific attenuation at horizontal and vertical polarizations have been introduced and expressed as functions of both Z_H and Z_{DR}, according to empirical relationships obtained by Aydin et al. (1986). The method they suggest for simulating radar measured reflectivities in each gate has also been adopted in our simulation.

Simulations have been carried over a 10 Km x 10 Km square area, for a precipitation event lasting 50 minutes, to generate an event sufficiently extended in time and space with an acceptable computing time. Generated rainfall fields are sampled over an uniformly 0.1 Km spaced grid, fixing the components $\bar{V}_x$ and $\bar{V}_y$ of the average velocity as 5 and 10 Km h^{-1} respectively.

The adopted values of the statistical rainfall model parameters allow the generation of quite severe precipitation events. Table 1 lists the values of parameters of performed radar simulation, d_R being the distance between radar and the reflectivity data volume.

Table 1

h_s(m)	d_R(Km)	ϵ(deg)	Φ_l(deg)	Φ_r(deg)	Δr(m)	N_i
660	45	0.5	2.2	0.9	150	64

A sequence of 50 scans separated by 1 minute intervals (antenna scan period) was obtained over the cited sector, each scan consisting of 11 rays (with azimuthal resolution Φ_r) each one consisting of 65 range resolution cells.

3. APPLICATION OF THE INTEGRATED MODEL

3.1 Test of an attenuation correction procedure

To remove the attenuation propagation effects from the data acquired by a C-band meteorological radar, a correction procedure must be applied. The simulation model can give some indications about the efficiency of a given procedure. The tested procedure is the iterative algorithm described by Aydin et al. (1988) for correction of absolute and differential attenuation effects. Such procedure has been applied setting standard deviations of the measurement errors N_{ZHn} and N_{ZDRn}, as 0.5

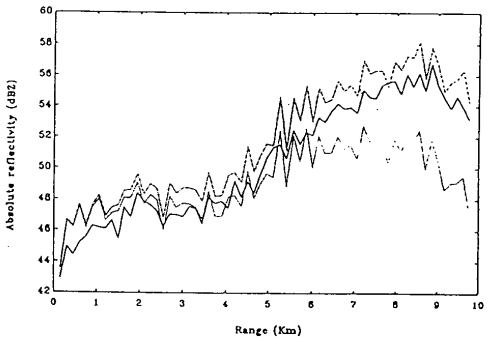

Fig. 2a Z_H as a function of range before introducing the effect of the attenuation and of the system errors (continuous curve), after their introduction (point curve), and after the attenuation correction procedure (hatched curve).

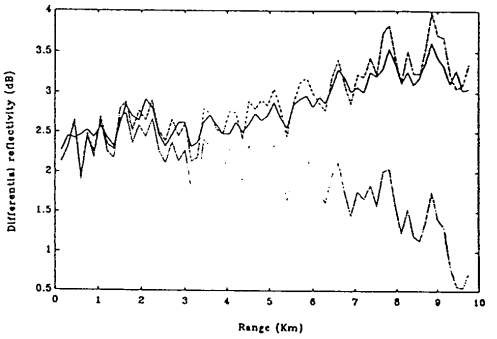

Fig. 2b Same as in figure 2, for Z_{DR}.

and 0.1 dB, respectively, and the biases due to calibration errors B_{ZH} and B_{ZDR}, as 1 dB and -0.1 dB respectively (the last refers to the greatest errors in the correction of radar reflectivities among three cases there considered). Figs. 2a and 2b that we report as an example show, for the same particular radar ray and the same scan, effects of the the introduction of the attenuation effect and the application of the correction procedure. It is easy to verify that the correction is quite good and that the major error depends on the initial bias.

3.2 Filtering of radar data

Filtering techniques should be performed to the required, spatially uniform, accuracy. Radar map corrupted by large clutter areas could be reconstructed by means of proper filtering techniques. Furthermore, image enhancement techniques are required as a pre-processing step for improving the performance of automatic cell detection and tracking algorithms. Substantially, filtering of the radar estimate allows to reduce the influence of random errors that cannot be removed by the raingage calibration. A radar reflectivity map can be modeled as a digital image corrupted both by structured background, signal dependent and independent, spatially non-stationary, noise with unknown statistics. For such cases, two kinds of filtering techniques have been considered factorily. Adaptive space-time filtering techniques are adequate for clutter removal, since are capable of identifying the dynamic structure of the event and allow adaptation on the local features of the noise field. Beside, they can also provide a very short term prediction, usable for hydrological applications. On the other hand, ranked-order filters, based on order statistics are widely employed in image processing, because they are capable to reduce effects due to several kinds of noise, while preserving edges. Here we present a comparison between some of these filtering algorithms. Reflectivity data are converted by bilinear interpolation in a Cartesian grid and converted into a ground rainfall map by (6). Resulting grid has a 10^{-2} Km^2 pixel resolution to exactly overlay ground "true" rainfall field map. Comparative results are carried out by using NB (Normalized Bias) and NSED (Normalized Standard Error of Difference), which give the average relative error over the covered area and the measure of spatial fluctuation of errors in the same area, respectively. The results thus obtained through the simulated data are reported in Table 2. They refer to the median filter(Arce et al., 1987), the max-median filter (Arce and McLoughlin, 1987), and the min-max filter (Werman and Peleg, 1985). Considering that NB = 29.0% and NSED = 39.5% refers to unfiltered estimates, the effectiveness in the reduction of NSED parameter is evident, as well as the introduction of further bias. Such bias can be reduced by means of calibration through raingage.

Table 2

	Median		Max/median		Min/max	
order	NB%	NSED%	NB%	NSED%	NB%	NSED%
1	34.7	35.6	38.3	37.5	35.1	32.6
2	38.7	32.8	46.7	36.5	39.9	29.5
3	42.7	30.9	52.2	35.6	45.7	27.7
4	45.7	29.0	60.7	33.8	49.6	27.5

3.3 Radar calibration through raingages

"Calibration" with raingage is the most common technique to adjust radar rainfall estimates. There are several methods conceived for this task. The proposed simulation scheme can give the opportunity to compare the performance of calibration techniques in a fully controlled experiment. Furthermore, it allows to optimize the choice of parameters of given method, such as the calibrating raingage density. Here we illustrate the application of the simulation scheme for evaluating an adjustment technique based upon the optimal choice of the rainfall-reflectivity relationship both for a dual polarization radar and a monoparametric radar operating in the same conditions. Such relationship are:

$$R = a\, Z_H^{\,b} \tag{7}$$

and

$$Z_H = A\, Z_{DR}\, R^B. \tag{8}$$

Rainfall depth raingage measurements were made available at each location, at the same time and every minute, by time integration of the "true" rainfall rate at ground, corrupted by an error of 5% on the "true" rainfall rate in terms of standard deviation. The parameters a, b, A, B have been computed by a linear regression method, performed on time window starting from the beginning of the event, during which raingage data have been integrated, and on N_r raingages. Nine locations were chosen such that N_r may vary the average density of the "calibration" network from a minimum of 1 gage per 100 Km^2 to a maximum of 1 gage per 11.1 Km^2. In order that the comparison with the monoparametric radar technique might be meaningful, we neutralized the negative effects that a bad estimate of Z_{DR} could have in the presence of attenuation by applying the correction algorithm only on the estimates of Z_H. Consequently, errors affecting the rain rate estimates, obtained by (7), are expected to be the lowest in the same operational conditions, since the use of Z_{DR} has surely positive effects on the correction of Z_H. Obtained results are illustrated in Figs. 3 and 4, where NB and NSED are

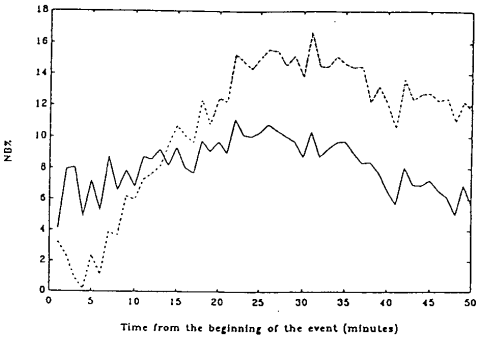

Fig. 3a NB for the error relative to the Z_{DR} technique (continuous line) and to the monoparametric technique (hatched line) computed for N_r=9 and T_i=10 min.

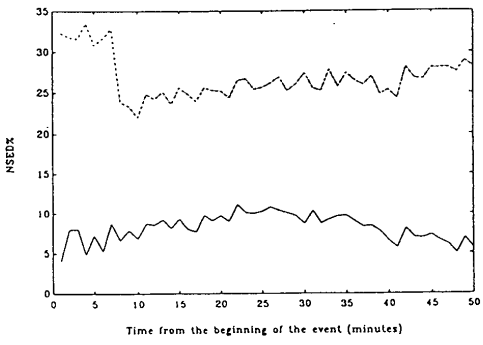

Fig. 3b NSED relative to the Z_{DR} technique (continuous line) and to the monoparametric technique (hatched line) computed for N_r=9 and T_i=10 min.

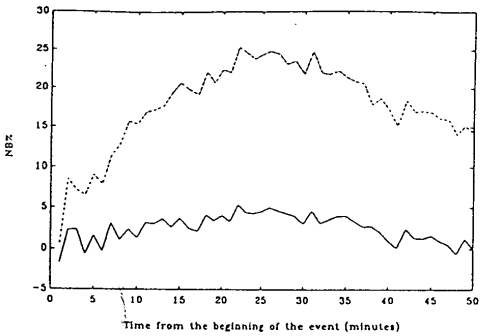

Fig. 4a As in figure 3a, but for N_r=4 T_j=50.

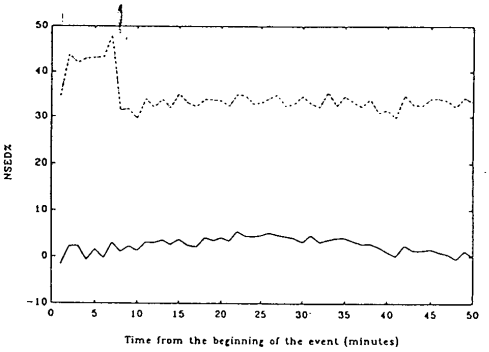

Fig. 4b As in figure 3b, but for N_r=4 T_j=50.

computed considering the gage measured rainfall as the "true" reference. Such figures show that the dual polarization radar exploits at the utmost its potential when A and B are derived with enough accuracy. We notice indeed that even when only one raingage is present, increasing T_j effectively improves the rainfall estimates. However the most appreciable results are achieved when more raingages are used, also for small values of T_j. This suggests that best fit relationships should be used that take into account the spatial variability of rainfall over the examined area, rather than its variations in time. This behavior seems to be confirmed by the fact that, if T_j overcomes a certain threshold (around 30 minutes), the trend of decreasing errors seems to stop or even to invert. In all cases with N_r=9, both NB and NSED are decidedly less for the Z_{DR} technique than for the single polarization method, in spite of the favorable attenuation compensation performed in the monoparametric radar.

4. ACKNOWLEDGEMENT

This work has been supported by the National Research Council (CNR) within the "Arno Project", funded through the National Group for the Defense from Hydrogeological Hazards and the Strategic Project "Arno".

5. REFERENCES

Arce, G.R., Gallagher, N.C., and T.A. Nodes, 1986: Median filters: theory for one- and two-dimensional filters. In T.S. Huang, Ed., *Advances in computer vision and image processing*, vol. 22. Greenwich, CT:JAI Press, 89-166.

Arce, G.R., and M.P. McLoughlin, 1987: Theoretical analysis of the max/median filter. *IEEE Trans. Acoust., Speech, Signal Processing*, vol. ASSP-35, pp. 60-69.

Atlas, D., Srivastava, R.C., and R.S. Sekhon, 1973: Doppler radar characteristics of precipitation at vertical incidence. *Rev. Geophys. Space Phys.*, 2, 1-35.

Aydin, K., Seliga, T.A. and Y. Zhao, 1986: A self-correction procedure of attenuation due to rain for C-band dual linear polarization radars. *Prep. 23rd Conf. on Radar Meteorology*, Snowmass, Colorado, Amer. Meteor. Soc., 3, pp JP337-JP341.

Aydin, K., Seliga, T. A. and Y. Zhao, 1988: Rain-induced attenuation effects on C-band dual-polarization meteorological radars. *IEEE Trans. Geosci. Remote Sensing*, GE-27, 1, pp 57-66.

Becchi, I. and D. Giuli, 1987: Description of the Arno Project: a real-time approach to the Arno river flooding forecast., *The records of the International Conference on the Arno Project*, Florence, Italy, GNDCI-29, pp 9-49.

Doviak, R.J. and Zrnić, D.S., 1984: *Doppler radar and weather observations*. Academic Press, New York.

Hall, M.P.M., Goddard, J.W.F., and S.M. Cherry, 1984: Identification of hydrometeors and other targets by dual polarization radar. *Radio Sci.*, 19, 132-140.

Marshall, J., S. and W. M. K. Palmer, 1948: The distribution of raindrops with size. *J. Meteor.*, 5, 165-166.

Rodriguez-Iturbe, I. and P.S. Eagleson, 1987: Mathematical models of rainstorm events in space and time. *Water Resources Res.*, 23, 181-190.

Sachidananda, M. and D.S. Zrnić, 1987: Rain rate estimates from differential reflectivity measurements. *J. Atmos. Ocean. Technol.*, 4, 588-598.

Seliga, T.A. and V.N. Bringi, 1976: Potential use of radar differential reflectivity measurements at orthogonal polarizations for measuring precipitation. *J. Appl. Meteorol.*, 15, 69-76.

Werman, M., and S. Peleg, 1985: Min-max operators in texture digital picture processing. *IEEE Trans. Pattern Anal. Machine Intell.*, vol. PAMI-7, 6, 730-733.